J|A|C|S
ARTICLES
Published on Web 08/27/2002

Insights into the Free-Energy Dependence of Intramolecular Dissociative Electron Transfers

Sabrina Antonello,[†] Marco Crisma,[‡] Fernando Formaggio,[‡] Alessandro Moretto,[‡] Ferdinando Taddei,[§] Claudio Toniolo,[‡] and Flavio Maran*[,†]

Contribution from the Dipartimento di Chimica Fisica, Università di Padova, via Loredan 2, 35131 Padova, Italy, Dipartimento di Chimica Organica, Istituto di Chimica Biomolecolare, C.N.R., Università di Padova, via Marzolo 1, 35131 Padova, Italy, and Dipartimento di Chimica, Università di Modena e Reggio Emilia, via Campi 183, 41100 Modena, Italy

Received March 29, 2002

Abstract: To study the relationship between rate and driving force of intramolecular dissociative electron transfers, a series of donor−spacer−acceptor (D−Sp−A) systems has been devised and synthesized. *cis*-1,4-Cyclohexanedyil and a perester functional group were kept constant as the spacer and acceptor, respectively. By changing the aryl substituents of the phthalimide moiety, which served as the donor, the driving force could be varied by 0.74 eV. X-ray diffraction crystallography and ab initio conformational calculations pointed to D−Sp−A molecules having the *cis*-(cyclohexane) equatorial(phthalimido)−axial(perester) conformation and the same D/A orientation. The intramolecular dissociative electron-transfer process was studied by electrochemical means in *N,N*-dimethylformamide, in comparison with thermodynamic and kinetic information obtained with models of the acceptor and the donor. The intramolecular process consists of the electron transfer from the electrochemically generated phthalimide-moiety radical anion to the peroxide functional group. The electrochemical analysis provided clear evidence of a concerted dissociative electron-transfer mechanism, leading to the cleavage of the O−O bond. Support for this mechanism was obtained by ab initio MO calculations, which provided information about the LUMO of the acceptor and the SOMO of the donor. The intramolecular rate constants were determined and compared with the corresponding intermolecular values, the latter data being obtained by using the model molecules. As long as the effective location of the centroid of the donor SOMO does not vary significantly by changing the aryl substituent(s), the intramolecular dissociative electron transfer obeys the same main rules already highlighted for the corresponding intermolecular process. On the other hand, introduction of a nitro group drags the SOMO away from the acceptor, and consequently, the intramolecular rate drops by as much as 1.6 orders of magnitude from the expected value. Therefore, a larger solvent reorganization than for intermolecular electron transfers and the effective D/A distance and thus electronic coupling must be taken into account for quantitative predictions of intramolecular rates.

Predicting the rate of chemical reactions as a function of driving force and environmental parameters is a challenging and stimulating task. In this connection, the most important achievements have been probably reached in the area of electron-transfer (ET) processes, thanks to the Marcus theory of outer-sphere ET and its subsequent implementations.[1] It is known that for some chemical systems ET is also liable to cause the cleavage of a σ bond, leading to formation of reactive species such as radicals and ions.[2,3] The dissociation of the frangible bond may follow or be even concerted to the ET itself. In the purely dissociative case (eq 1, where the electron is provided by any

$$AB + e \rightarrow A^{\bullet} + B^{-} \qquad (1)$$

suitable donor), the reaction proceeds along a reaction coordinate that, for the most common case of reduction of a neutral compound, does not involve the transient formation of the radical anion, which rests on a more energetic potential energy surface. As a rule, the concerted dissociative ET (DET) reaction is thermodynamically favored over the corresponding stepwise process when the standard potential for the formation of the radical anion is sufficiently negative and the cleaving bond is weak, such as with peroxides,[4−7] or when a good leaving group forms, such as with alkyl halides.[3,8−10] In fact, by using a thermochemical cycle, the standard potential (E°) of a concerted

* To whom correspondence should be addressed. Tel: +39 (049) 827-5147. Fax: +39 (049) 827-5135. E-mail: f.maran@chfi.unipd.it.
[†] Dipartimento di Chimica Fisica, Università di Padova.
[‡] Dipartimento di Chimica Organica, Università di Padova.
[§] Università di Modena e Reggio Emilia.

(1) For example, see: (a) Marcus, R. A.; Sutin, N. *Biochim. Biophys. Acta* **1985**, *811*, 265. (b) Eberson, L. *Electron-Transfer Reactions in Organic Chemistry;* Springer-Verlag: New York, 1987. (c) *Electron Transfer: From Isolated Molecules to Biomolecules*; Jortner, J., Bixon, M., Eds.; Wiley: New York, 1999; Part 1.
(2) Maran, F.; Wayner, D. D. M.; Workentin, M. S. *Adv. Phys. Org. Chem.* **2001**, *36*, 85.
(3) Savéant, J.-M. *Adv. Phys. Org. Chem.* **2000**, *35*, 117.
(4) (a) Workentin, M. S.; Maran, F.; Wayner, D. D. M. *J. Am. Chem. Soc.* **1995**, *117*, 2120. (b) Antonello, S.; Musumeci, M.; Wayner, D. D. M.; Maran, F. *J. Am. Chem. Soc.* **1997**, *119*, 9541. (c) Donkers, R. L.; Maran, F.; Wayner, D. D. M.; Workentin, M. S. *J. Am. Chem. Soc.* **1999**, *121*, 7239.

DET can be expressed as a function of the bond dissociation free energy (BDFE) of the cleaving bond and the $E°$ of the leaving group:[2]

$$E^{\circ}_{AB/A^{\bullet},B^{-}} = E^{\circ}_{B^{\bullet}/B^{-}} - \mathrm{BDFE}/F \qquad (2)$$

What characterizes concerted DETs is that they are energetically very demanding and thus intrinsically slow processes. This is because of their large intrinsic barrier ($\Delta G_0^{\ddagger}$), which is the activation free energy ($\Delta G^{\ddagger}$) at $\Delta G° = 0$. In fact, concerted DETs requires significant stretching of the cleaving bond as the reacting system evolves toward the transition state. Savéant developed a simple but nevertheless very useful model to describe these ET reactions and showed that, besides the usual solvent reorganization energy, one-fourth of the bond dissociation energy (BDE) of the cleaving bond contributes to determining $\Delta G_0^{\ddagger}$.[11] In its most used and practical form, the model leads to a quadratic $\Delta G^{\ddagger} - \Delta G°$ relationship that is formally identical to the well-known Marcus equation. Thus, the adiabatic DET rate constant expression can be simply written as

$$k = Z \exp\left[-\frac{\Delta G_0^{\ddagger}}{RT}\left(1 + \frac{\Delta G^{\circ}}{4\Delta G_0^{\ddagger}}\right)^2\right] \qquad (3)$$

Besides $\Delta G_0^{\ddagger}$, concerted DETs may also be slow for other reasons. In particular, we have recently shown that the actual prefactor of DETs can be much smaller than the value Z expected for an adiabatic process characterized by the same $\Delta G_0^{\ddagger}$ and studied in the same $\Delta G°$ range.[4,6,7] This behavior was hypothesized to be related to the failure of the Born−Oppenheimer approximation near the transition state,[7] which would cause the avoided crossing of the reactant and product curves to be only narrowly avoided.[12] In conclusion, because of small preexponential values (which cause the log k vs $\Delta G°$ curve to shift downward) and/or large $\Delta G_0^{\ddagger}$s (which flattens the parabola), the rate constants of concerted DETs are smaller and much less sensitive to $\Delta G°$ changes than observed with common nondissociative outer sphere ETs. The most important conclusion, however, is that, once these factors are taken into account, the shape of the log k versus $\Delta G°$ relationship and thus the value of k at any given $\Delta G°$ value can be predicted satisfactorily.

In recent years several groups have collected data and provided relevant insights into the dynamics of intermolecular DETs, as recently reviewed.[2,3,8,9,11b] On the other hand, less information is available on the corresponding intramolecular processes. Indeed, interesting results and analyses of the decay of radical anions occurring by fragmentation of a σ bond have been published.[2,3,8,11b,13−24] Except for a few systems,[21−24] however, the antibonding orbital initially hosting the electron (most often a π^* orbital) is often very strongly coupled to the σ^* orbital of the cleaving bond, which makes the description of the overall process in terms of electron uptake followed by intramolecular $\pi^* \rightarrow \sigma^*$ ET as not quite realistic.[25] On the other hand, it is well known that fascinating results have been obtained in the area of intramolecular nondissociative ETs, leading to the building of a sound experimental−theoretical framework to understand how electrons are transferred through bonds and space.[1c,26] This knowledge was reached by using well-devised D−Sp−A molecular systems, in which a donor (D) and an acceptor (A) are spatially separated by a spacer (Sp) having specifically tailored properties. Very recently, we studied the $\Delta G°$ dependence of intramolecular DETs in D−Sp−A molecules (eq 4) in which a tertiary bromide functional group was

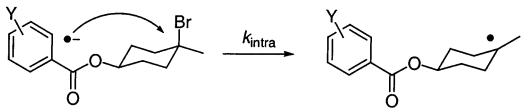

(4)

chosen as the acceptor, ring-substituted benzoates were the donors, and cyclohexyl was the spacer.[24] For these systems, comparison of the intramolecular and the intermolecular log k versus $\Delta G°$ plots revealed that the intramolecular rate constants are more sensitive to variation of $\Delta G°$ than observed for the bimolecular reaction. Typically, when the driving force was decreased by ~15 kcal mol^{-1}, the rate was found to drop 1 order of magnitude more rapidly than expected. This experi-

(5) (a) Donkers, R. L.; Workentin, M. S. *J. Phys. Chem. B* **1998**, *102*, 4061. (b) Workentin, M. S.; Donkers, R. L. *J. Am. Chem. Soc.* **1998**, *120*, 2664. (c) Magri, D. C.; Donkers, R. L.; Workentin, M. S. *J. Photochem. Photobiol. A: Chem.* **2001**, *138*, 29. (b) Donkers, R. L.; Workentin, M. S. *Chem. Eur. J.* **2001**, *7*, 4012.
(6) (a) Antonello, S.; Maran, F. *J. Am. Chem. Soc.* **1997**, *119*, 12595. (b) Antonello, S.; Maran, F. *J. Am. Chem. Soc.* **1999**, *121*, 9668.
(7) Antonello, S.; Formaggio, F.; Moretto, A.; Toniolo, C.; Maran, F. *J. Am. Chem. Soc.* **2001**, *123*, 9577.
(8) Eberson, L. *Acta Chem. Scand.* **1999**, *53*, 751.
(9) Lund, H.; Daasbjerg, K.; Lund, T.; Pedersen, S. U. *Acc. Chem. Res.* **1995**, *28*, 313.
(10) (a) Andrieux, C. P.; Gallardo, I.; Savéant, J.-M.; Su, K. B. *J. Am. Chem. Soc.* **1986**, *108*, 638. (b) Savéant, J.-M. *Adv. Phys. Org. Chem.* **1990**, *26*, 1. (c) Savéant, J.-M. *J. Am. Chem. Soc.* **1992**, *114*, 10595.
(11) (a) Savéant, J.-M. *J. Am. Chem. Soc.* **1987**, *109*, 6788. (b) Savéant, J.-M. In *Advances in Electron-Transfer Chemistry*; Mariano, P. S., Ed.; JAI Press: Greenwich, CT, 1994; Vol. 4, p 53. (c) Andrieux, C. P.; Savéant, J.-M.; Tardy, C. *J. Am. Chem. Soc.* **1998**, *120*, 4167.
(12) Butler, L. J. *Annu. Rev. Phys. Chem.* **1998**, *49*, 125.
(13) (a) Maslak, P. In *Topics in Current Chemistry*; Mattay, J., Ed.; Springer-Verlag: Berlin, 1993; Vol. 168, p 1. (b) Maslak, P.; Vallombroso, T. M.; Chapman, W. H., Jr.; Narvaez, J. N. *Angew. Chem., Int. Ed. Engl.* **1994**, *33*, 73.
(14) (a) Severin, M. G.; Arévalo, M. C.; Maran, F.; Vianello, E. *J. Phys. Chem.* **1993**, *97*, 150. (b) Daasbjerg, K.; Jensen, H.; Benassi, R.; Taddei, F.; Antonello, S.; Gennaro, A.; Maran, F. *J. Am. Chem. Soc.* **1999**, *121*, 1750. (c) Antonello, S.; Benassi, R.; Gavioli, G.; Taddei, F.; Maran, F. *J. Am. Chem. Soc.* **2002**, *124*, 7529.
(15) (a) Savéant, J.-M. *J. Phys. Chem.* **1994**, *98*, 3716. (b) Andrieux, C. P.; Robert, M.; Savéant, J.-M. *J. Am. Chem. Soc.* **1995**, *117*, 9340. (c) Andrieux, C. P.; Savéant, J.-M.; Tallec, A.; Tardivel, R.; Tardy, C. *J. Am. Chem. Soc.* **1996**, *118*, 9788. (d) Andrieux, C. P., Savéant, J.-M.; Tallec, A.; Tardivel, R.; Tardy, C. *J. Am. Chem. Soc.* **1997**, *119*, 2420. (e) Andrieux, C. P., Combellas, C.; Kanoufi, F.; Savéant, J.-M.; Thiébault, A. *J. Am. Chem. Soc.* **1997**, *119*, 9527.
(16) (a) Andersen, M. L.; Mathivanan, N.; Wayner, D. D. M. *J. Am. Chem. Soc.* **1996**, *118*, 4871. (b) Andersen, M. L.; Long, W.; N.; Wayner, D. D. M. *J. Am. Chem. Soc.* **1997**, *119*, 6590. (c) Andersen, M. L.; Wayner, D. D. M. *Acta Chem. Scand.* **1999**, *53*, 830.
(17) (a) Christensen, T. B.; Daasbjerg, K. *Acta Chem. Scand.* **1997**, *51*, 307. (b) Jakobsen, S.; Jensen, H.; Pedersen, S. U.; Daasbjerg, K. *J. Phys. Chem. A* **1999**, *103*, 4141. (c) Enemærke, R. J.; Christensen, T. B.; Jensen, H.; Daasbjerg, K. *J. Chem. Soc., Perkin Trans. 2* **2001**, 1620.
(18) Tanko, J. M.; Phillips, J. P. *J. Am. Chem. Soc.* **1999**, *121*, 6078.
(19) Zheng, Z.-R.; Evans, D. H.; Chan-Shing, E. S.; Lessard, J. *J. Am. Chem. Soc.* **1999**, *121*, 9429.
(20) Janssen, R. G.; Utley, J. H. P., Carré, E.; Simon, E.; Schirmer, H. *J. Chem. Soc., Perkin Trans. 2* **2001**, 1573.
(21) (a) Pearl, D. M.; Burrow, P. D.; Nash, J. J.; Morrison, H.; Jordan, K. D. *J. Am. Chem. Soc.* **1993**, *115*, 9876. (b) Pearl, D. M.; Burrow, P. D.; Nash, J. J.; Morrison, H.; Nachtigallova, D.; Jordan, K. D. *J. Phys. Chem.* **1995**, *99*, 12379.
(22) (a) Kimura, N.; Takamuku, S. *Bull. Chem. Soc. Jpn.* **1991**, *64*, 2433. (b) Kimura, N.; Takamuku, S. *Bull. Chem. Soc. Jpn.* **1992**, *65*, 1668. (c) Kimura, N.; Takamuku, S. *J. Am. Chem. Soc.* **1994**, *116*, 4087. (d) Kimura, N.; Takamuku, S. *J. Am. Chem. Soc.* **1995**, *117*, 8023. (e) Kimura, N. *J. Am. Chem. Soc.* **2001**, *123*, 3824.
(23) Addock, W.; Andrieux, C. P.; Clark, C. I.; Neudeck, A.; Savéant, J.-M.; Tardy, C. *J. Am. Chem. Soc.* **1995**, *117*, 8285.
(24) Antonello, S.; Maran, F. *J. Am. Chem. Soc.* **1998**, *120*, 5713.
(25) Burrow, P. D.; Gallup, G. A.; Fabrikant, I. I.; Jordan, K. D. *Aust. J. Phys.* **1996**, *49*, 403.
(26) For example, see: (a) Closs, G. L.; Miller, J. R. *Science* **1988**, *240*, 440. (b) Paddon-Row; M. N. *Acc. Chem. Res.* **1994**, *27*, 18.

mental outcome was explained by the hypothesis that the effective distance at which the intramolecular ET takes place changes when the driving force is varied. Since $\Delta G°$ is increased by introducing a more-electron-withdrawing Y substituent, for example, by replacing the para hydrogen with a cyano group, an increase of the effective distance for the least exergonic reactions was thus attributed to a shift of the centroid of the donor π^* orbital, in which the unpaired electron is initially located, away from the acceptor. This subtle distance effect on the ET rate would be forcefully absent in intermolecular ETs, where random distance and orientation distributions in the encounter complex yield to measure an average ET rate constant.

This type of effect, which should not depend on whether the acceptor undergoes bond cleavage or not, reduces our ability to predict the rate of a given intramolecular ET reaction for different $\Delta G°$ values. The aim of this paper is to shed new light onto this still unexplored issue, which goes beyond the commonly employed concepts of edge-to-edge or center-to-center D/A distance. To obtain a better description of the rate−driving force relationship ruling intramolecular DETs and also to obtain a more detailed interpretation of the distance effect on ET processes, we synthesized the series of compounds **1a**−**e** in which the distance and orientation of the exchanging centers is kept reasonably well controlled. We also synthesized compounds **1f** and **1g**, for which significant differences were expected. Substituted phthalimido moieties were chosen as the donors. For **1a**−**e**, the substituents were selected to provide less chance to observe the above-mentioned trend of the bromide systems. The perester functional group RCO_2−O*t*Bu, a well-defined dissociative-type acceptor,[6,7] and cyclohexyl were kept constant as the acceptor and the spacer, respectively. The D−Sp−A compounds **1a**−**g** were studied in comparison with the thermodynamic and kinetic information obtained with the model acceptor **2**, the corresponding model donors **3a**−**g**, and their carboxylic acid precursors **4a**−**g**. X-ray diffraction crystallography and ab initio conformational calculations pointed to D−Sp−A molecules having the *cis*-(cyclohexane) equatorial-(phthalimido)−axial(perester) conformation and the same D/A orientation. Further theoretical calculations, aimed at understanding the energetics and nature of the relevant orbitals, provided information about the LUMO of the acceptor, as a function of the O−O bond elongation, and the singly occupied molecular orbital (SOMO) of the donor. We determined both the intra- and the intermolecular log *k* versus $\Delta G°$ relationships of DET in *N*,*N*-dimethylformamide (DMF) using electrochemical methods. By exploiting this strategy, we could prove that

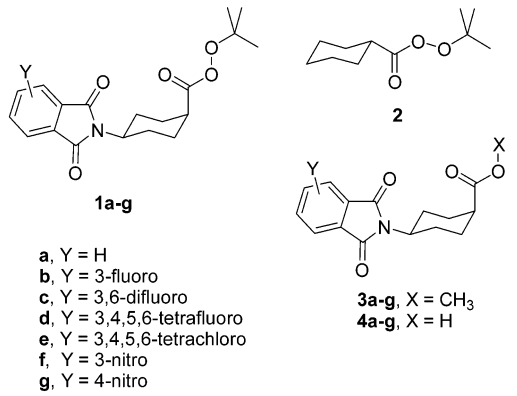

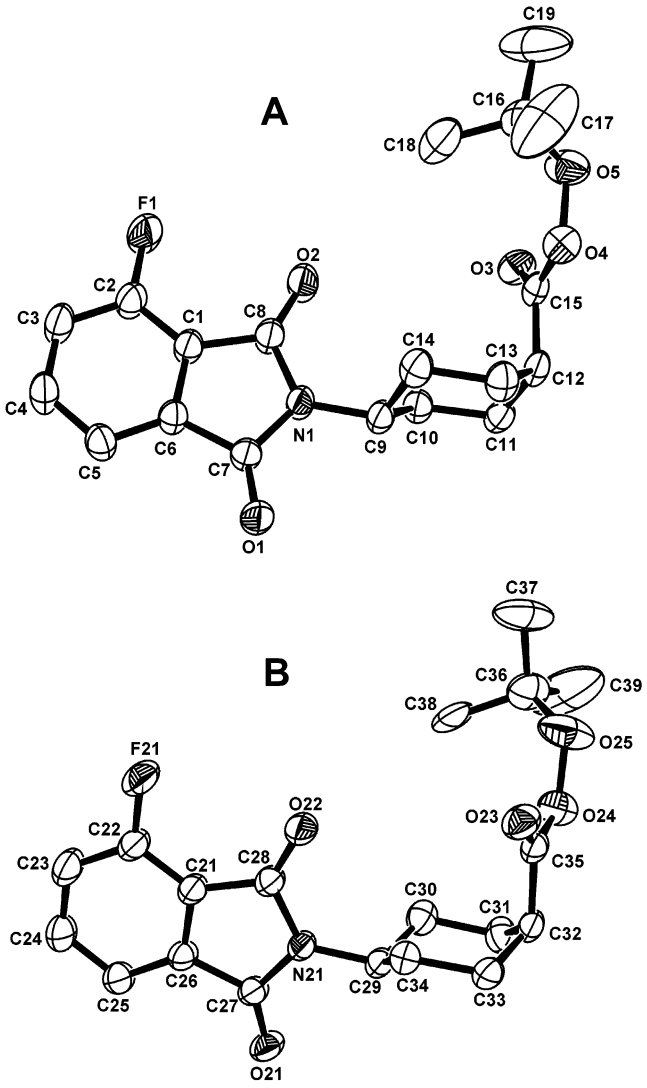

Figure 1. X-ray diffraction structures of **1b** (see text). Displacement ellipsoids are drawn at the 30% probability level. For clarity, only one position is shown for the disordered *t*Bu group of molecule **B**.

the intramolecular DET obeys the same rules already highlighted for the corresponding intermolecular process. However, in general, a larger solvent reorganization energy and the effective D/A distance must be taken into account for quantitative predictions.

Results and Discussion

Structural Analysis and ab Initio Conformational Calculations. Single crystals of **1a**−**c** were analyzed by X-ray diffraction crystallography. The conformational features of **1a**, **1b** (two independent molecules, A and B), and **1c** are quite similar. Figure 1 illustrates both structures A and B of **1b**. In all structures, the cyclohexyl ring is found in the chair disposition, with the following puckering parameters:[27] **1a**, Q_T = 0.559(2) Å and θ_2 = 177.0(2)°; **1b** A, Q_T = 0.559(3) Å and θ_2 = 177.0(3)°; **1b** B, Q_T = 0.555(3) Å and θ_2 = 177.4(3)°; **1c** Q_T = 0.568(4) Å and θ_2 = 176.0(4)°. The phthalimido and perester substituents are in the equatorial and axial positions, respectively. The plane of the phthaloyl moiety is almost perpendicular to the plane of the cyclohexyl ring (taken as, for

(27) Cremer, D.; Pople, J. A. *J. Am. Chem. Soc.* **1975**, *97*, 1354.

example, the C10−C11−C13−C14 plane), the dihedral angles are as follows: **1a**, 80.6(1)°; **1b** A, 85.1(1)°; **1b** B, 83.5(1)°; **1c**, 89.7(1)°. With respect to the same cyclohexyl plane, the dihedral angles of the perester sp^2 system are as follows: **1a**, 82.3(1)°; **1b** A, 82.5(1)°; **1b** B, 83.2(1)°; **1c**, 86.1(1)°. However, the O3 carbonyl oxygen atom of the perester group (for **1b** B, O23) is syn-periplanar to the C11 carbon atom (or C33), the C9−C12−C15−O3 (or C29−C32−C35−O23) torsion angles being as follows: **1a**, −62.3(3)°; **1b** A, −71.3(3)°; **1b** B, 77.6(3)°, **1c**, −63.7(5)°. Finally, the O−O bond is almost parallel to the normal to the cycloxehyl plane and perpendicular to that of the phthaloyl system, the corresponding angles being, respectively, as follows: **1a**, 7.4(1) and 78.0(1)°; **1b** A, 3.8(1) and 84.7(1)°; **1b** B, 4.7(2) and 81.9(1)°; **1c**, 4.9(2) and 87.1(1)°.

Ab Initio MO calculations were carried out at the HF/6-31G*//HF/6-31G* level on both equatorial and axial *N*-cyclohexyl phthalimide **5**. The orientation of the phthaloyl plane with respect to the plane of the cyclohexyl ring is consistent with the data from the crystal structures, the torsion angle now being 90°. Although it is known that the equatorial conformation of esters (methyl and ethyl) of cyclohexanecarboxylic acid is only 1.1−1.3 kcal mol^{-1} more stable than the axial conformation,[28] we found that for *N*-cyclohexyl phthalimide the equatorial conformation is favored by as much as 5.83 kcal mol^{-1}. Therefore, with reference to **1a**−**g**, we may conclude that inversion of the *cis*-(cyclohexane) equatorial(phthalimido)−axial(perester) conformation should be energetically quite unlikely.

A further aspect, related to the donor/acceptor distance, was considered. We studied another model molecule, methyl *cis*-4-maleimidocyclohexanepercarboxylate **6**, at the HF/6-31G*//HF/

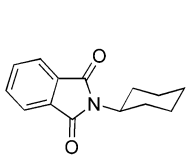

5

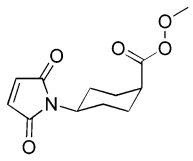

6

6-31G* level. This system minimizes its energy by adopting the equatorial(maleimido)−axial(methyl perester) conformation, in analogy with the X-ray diffraction data of **1a**−**c**. The calculations showed that the perester C═O is oriented with respect to the cyclohexyl ring exactly as shown by X-ray crystallography for **1a**−**c**. It appears that some interaction between the C═O group and one of the axial hydrogens at either the 3- or 5-position (according to the calculations and the X-ray diffraction data, this distance is 2.66 and 2.5−2.7 Å, respectively) could be responsible for this stabilization. Although the energy increases only slightly, 1.3 kcal mol^{-1}, when the C═O is directed exactly toward the donor moiety, when the perester C═O is forced outward, the cyclohexyl ring the increase is 2.3 kcal mol^{-1}. These results suggest that the main contribution to the intramolecular ET (see below) comes from the same geometrical arrangement already illustrated in Figure 1. This implies that the D−Sp−A system adopts a well-defined and essentially fixed orientation and D/A distance. For the sake of the present investigation, it is particularly worth noting that there

(28) Eliel, E. L.; Wilen, S. H. *Stereochemistry of Organic Compounds*; Wiley: New York, 1994; Chapter 11.

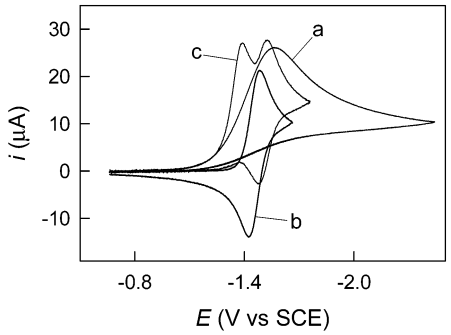

Figure 2. Background-subtracted cyclic voltammetries for the reduction of 1 mM **2** (curve a), **3a** (curve b), and **1a** (curve c) in DMF/0.1 M TBAP. Glassy carbon electrode, 0.2 V s^{-1}, and $T = 25$ °C.

are no reasons to believe that this scenario should depend on the remote phthaloyl substituents, as inferred from the X-ray diffraction data.

Direct Reduction of the Model Molecules. The cyclic voltammetric experiments were carried out at 25 °C in DMF containing 0.1 M tetrabutylammonium perchlorate (TBAP), using glassy carbon microelectrodes. The reduction of **2** is characterized by an irreversible and broad peak (Figure 2, curve a), having peak potential $E_p = -1.50$ V (at 0.2 V s^{-1}). The reduction entails a slow two-electron process and the formation of two oxidation peaks, detectable on the reverse positive-going scan. These peaks are generated by the oxidation of the two fragments of the dissociative ET, namely, tBuO$^-$ (E_p at ∼−0.25 V) and cyclohexylcarboxylate anion ($E_p = 0.99$ V). As previously described,[7] convolution analysis[6,29] of the voltammetric reduction peak of **2** allowed us to estimate the heterogeneous intrinsic barrier, $\Delta G_0^{\ddagger} = 13.3$ kcal mol^{-1}, the standard rate constant, $k^{\circ}_{het} = 9 \times 10^{-11}$ cm s^{-1}, and the E° of the process, −0.24 V. In analogy to what was found with a very similar molecule, *tert*-butyl pivaloyl perester,[7] both $\Delta G_0^{\ddagger}$ and E° are in very good agreement with the values 12.7 kcal mol^{-1} and −0.29 V obtained by applying the DET theory.[30] This agreement confirms the concertedness of the reduction mechanism and thus provides the conceptual basis to understand the large activation overpotential (∼1.2 V) suffered by the initial electron uptake. The DET yields the carboxylate ion and the tBuO$^{\bullet}$ radical directly at the electrode surface; the latter is thus rapidly reduced to tBuO$^-$, its E° being −0.23 V.[4a]

The reductions of **3a**−**g** and the conjugate bases of acids **4a**−**g** are electrochemically and chemically reversible (e.g., Figure 2, curve b), which allows straightforward determination of their E° values. The E° values and the k°_{het} values of **3a**−**g** are collected in Table 1. The k°_{het} values were calculated from the dependence of the peak-to-peak separation on the scan rate

(29) Imbeaux, J. C.; Savéant, J.-M. *J. Electroanal. Chem.* **1973**, *44*, 169.

(30) The BDE of **2** is assumed to be equal to the activation enthalpy for thermal decomposition**,** 32.4 kcal mol^{-1} [30a] (a theoretical estimation provided 30 kcal mol^{-1}: Benassi, R.; Taddei, F. *J. Mol. Struct.* **1994**, *303*, 101); this value can be converted to the BDFE at 25 °C (26.4 kcal mol^{-1}) by taking into account both the commonly used entropy factors[4] and the experimental activation entropy for thermal decomposition.[30a] As previously described for similar anions,[6b,7] voltammetric analysis of the oxidation peak of the carboxylate moiety of **4a** led us to estimate $E^{\circ} = 0.85$ V. Thus, E° was estimated (eq 2) to be −0.29 V. $\Delta G_0^{\ddagger}$ was estimated by combining the BDE value and a solvent reorganization energy of 18.4 kcal mol^{-1} (from the empirical equation $\lambda_S = 55.7/r$,[4b] where λ_S is given in kcal mol^{-1} and the molecular radius r in Å; r was obtained from the diffusion coefficient, 9.0×10^{-6} cm^2 s^{-1}, and the Stokes−Einstein equation). (a) Wolf, R. A.; Migliore, M. J.; Fuery, P. H.; Gagnier, P. R.; Sabeta, I. C.; Trocino, R. J. *J. Am. Chem. Soc.* **1978**, *100*, 7967.

Table 1. Voltammetric Data for the Reduction of **3a**−**g**, **4a**−**g**, and Corresponding Anions in DMF at 25 °C.

3	$E°$(**3**)[a] (V)	$k°_{het}$ (**3**)[b] ($cm^{-1}\,s^{-1}$)	$E°$(**4**)[a] (V)	$E°$(anion)[a] (V)
a	−1.447	0.12	−1.457	−1.496
b	−1.313	0.12	−1.321	−1.361
c	−1.175	0.14	−1.182	−1.221
d	−1.068	0.08	−1.080	−1.110
e	−0.979	0.11	−0.982	−1.010
f	−0.876	0.08	−0.891	−0.897
g	−0.709	0.10	−0.711	−0.719

[a] Calculated as the midpoint potential between the reduction and the oxidation peaks. [b]Calculated according to the Nicholson theoretical curve.[31]

according to the Nicholson's theoretical curve.[31] The results are in agreement with fast heterogeneous reductions and a substituent effect spanning a range of 0.74 V. A similar $E°$ range was observed with **4a**−**g** (0.75 V) and the corresponding carboxylates (0.78 V). Interestingly, the $E°$s of **4a**−**g** are no more than 0.01 V more negative than those of the corresponding **3a**−**g**; because of the negative charge, those of the carboxylates are more negative by 0.01−0.05 V. This observation is important because it stresses the efficiency of the cyclohexyl spacer in isolating the redox properties of the donor moiety from the nature of the other end of the molecule. In turn, it ensures that in the D−Sp−A compounds **1a**−**g** the $E°$s of both A and D should be the same of those of the model molecules **2** and **3a**−**g**.

Mediated Reduction of Perester 2. The intermolecular ET between **2** and the radical anions of the model donors **3a**−**g** were determined by using the redox catalysis approach.[32] In this method, the reversible reduction peak of the donor is transformed into an irreversible catalytic peak when the acceptor **2** is added to the solution. The catalytic reduction is based on the sequence described in eqs 5−8

$$D + e \rightleftarrows D^{\bullet -} \quad (5)$$

$$D^{\bullet -} + RCO_2{-}OtBu \rightarrow D + RCOO^- + tBuO^{\bullet} \quad (6)$$

$$D^{\bullet -} + tBuO^{\bullet} \rightarrow D + tBuO^- \quad (7)$$

$$tBuO^{\bullet} \xrightarrow{DMF} tBuOH \quad (8)$$

The ET rate constant (k_{inter}) values (Table 2) were obtained from simulation of the experimental curves obtained for each system at different scan rates and acceptor/donor molar ratios. Besides steps 5−7, the simulations included other side reactions that may affect the reduction of peroxides forming tBuO$^{\bullet}$.[4a,c,33] We found, however, that the reaction of tBuO$^{\bullet}$ with DMF (eq 8) is the main reaction path following the ET step 6. In agreement with the estimate that the ensuing DMF radical should be reducible at more negative potential,[33] we found the mediated reduction to be essentially a one-electron process. Different donors such as methyl *p*-nitrobenzoate and *p*-cyanobenzaldehyde provided log k_{inter} values in full agreement with those obtained with **3a**−**g**, indicating that the most important parameter to determine k_{inter} is only the donor $E°$. Overall, the results obtained for the mediated reduction of **2** are in very good agreement (i.e., they provide the same log k_{inter} vs $E°_{D/D^{\bullet -}}$ slope) with the results previously obtained with two other peresters having similar DET $E°$, namely, *tert*-butyl pivaloyl perester[7] and *tert*-butyl peracetate.[33]

Electrolysis of 1a. Compound **1a** was exhaustively reduced under potentiostatic conditions. The potential was controlled at ∼−1.4 V, which corresponds to a potential slightly more positive than that of the first peak of **1a** (cf. Figure 2, curve c). Acetanilide was added as a weak acid to the solution to prevent possible father−son reactions between the tBuO$^-$ anion and the unreacted peroxide, as found with similar peresters.[6] The progressive disappearance of the starting material was checked by running cyclic voltammetry experiments in the partially electrolyzed solution. After consumption of 1 F mol^{-1}, the irreversible peak was no longer evident and only the reversible peak corresponding to the reduction of the carboxylate anion was observed. This peak and that pertaining to carboxylate oxidation were the only voltammetric peaks detected in the available potential window. Noteworthy, the oxidation peak of the anion of acetanilide, which was expected at 0.08 V, was not detected, indicating that acetanilide was not acting as a proton donor toward the strong base tBuO$^-$.[34] This finding, together with the coulometric result, indicates that the main reaction of tBuO$^{\bullet}$ is H-atom abstraction from the solvent, in agreement with the above-mentioned catalysis result.[35]

After electrolysis, methyl iodide (2 equiv) was added to the solution to transform the carboxylate into the methyl ester **3a**. In less than 5 min. the alkylation was complete, as revealed by the transformation of the peak of the anion of **4a** (Figure 2, curve c, second peak) into that of **3a** (Figure 2, curve b). GC/MS also revealed the quantitative transformation into **3a**, which provided the expected fragmentation pattern. Quantitative analysis was carried out in comparison with an authentic sample of **3a**. In conclusion, we found that the reaction undergone by the radical anion of **1a** is an uncomplicated intramolecular dissociative ET (eqs 9 and 10). The absence of electrochemically

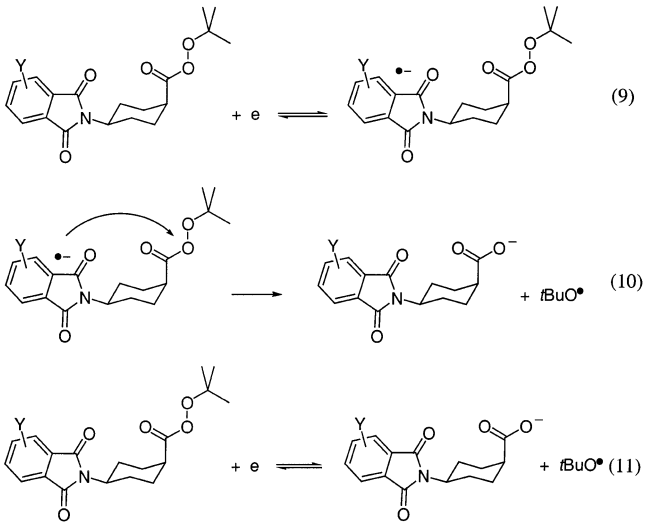

significant reactions of the tBuO$^{\bullet}$ radical or ensuing species

(31) Nicholson, R. S. *Anal. Chem.* **1965**, *37*, 1351.
(32) (a) Andrieux, C. P.; Blocman, C.; Dumas-Bouchiat, J. M.; M'Halla, F.; Savéant J.-M. *J. Electroanal. Chem.* **1980**, *113*, 19. (b) Andrieux, C. P.; Savéant J.-M. *J. Electroanal. Chem.* **1986**, *205*, 43.
(33) Kjær, N. T.; Lund, H. *Acta Chem. Scand.* **1995**, *49*, 848.
(34) The pK_a^{DMF} of acetanilide and tBuOH are 22.3 and 32.5, respectively.[34a,b] (a) Bordwell, F. G. *Acc. Chem. Res.* **1988**, *21*, 456. (b) Maran, F.; Celadon, D.; Severin, M. G.; Vianello, E. *J. Am. Chem. Soc.* **1991**, *113*, 9320.

simplifies the kinetic analysis of the intramolecular reaction (see below).

Intramolecular ET. In Figure 2, the cyclic voltammetry of **1a** is compared to those of **2** and **3a**. The first peak of **1a** is irreversible, in keeping with the reactivity of the initially electrogenerated radical anion (eq 9) to form the carboxylate anion and *t*BuO• radical (eq 10). The second peak is due to the reduction of the phthaloyl moiety in the carboxylate, as verified in comparison with an authentic sample of the conjugate base of **4a**. Some competition between direct (eq 11) and indirect (eqs 9 and 10) reduction of the perester end of **1a** is possible at low scan rates. As previously described in detail for a similar perester,[7] this competition is detectable at the foot of the wave, which is rather broad, and by studying the scan rate dependence of the peak width.[6] On the other hand, the competition becomes less evident and then disappears as the donor moiety becomes more easily reducible, the $E°$ of the acceptor being always the same. This is illustrated in Figure 3, in which the cyclic voltammetries of **1a**−**g** are compared. What is particularly worth noting in this figure is that the separation between the first and second peaks diminishes on going along the series from **1a** to **1e**. Moreover, the amount of formed carboxylate also decreases. Both features are in agreement with the occurrence of an increasingly slower intramolecular DET (eq 10). For **1f** and **1g**, reoxidation of the electrogenerated radical anion is detectable on the positive-going backward scan.

The voltammetric analysis of **1a**−**g** was based on the following evidence. The $E°$ of the donor and acceptor moieties in the D−Sp−A system are the same as those of the model molecules. In particular, the $E°$ of **1e**−**g** could be determined directly when the scan rate was increased at sufficiently high scan rates to reach reversible behavior. These observations ensure that the $\Delta G°$s of the intramolecular ET and corresponding intermolecular reaction are equal. Both reactions are uncomplicated concerted DET reactions, the only difference being that the mediator is either attached to the same molecular framework bearing the acceptor or freely diffusing with respect to the acceptor. The products are the unreactive carboxylate anion and the *t*BuO• radical, which rapidly abstracts an H-atom from the solvent. Although the competition between direct DET and indirect intramolecular DET complicates to some extent the voltammetric analysis aimed at obtaining the k_{intra} values of **1a**, **1b**, and **1c**, the problem is easily solved thanks to knowledge of the $E°$s and $k°_{het}$ values of **2**, **3a**−**c**, and the anions of **4a**−**c**. Furthermore, because of the very different intrinsic barriers involved, the indirect reduction mechanism (eqs 9 and 10) is favored over the concerted DET (eq 11) at larger driving forces, i.e., when E becomes more negative. This is conveniently accomplished by increasing the voltammetric scan rate, as previously discussed.[6,7]

To determine the k_{intra} values, the competitive intermolecular process, in which the perester of a D−Sp−A molecule is reduced by the radical anion of another molecule, was accounted for by using the k_{inter} values determined by redox catalysis. In addition, the reduction of **1a**−**g** was also studied as a function of concentration in the range 0.1−2 mM. These experiments allowed us to verify that the k_{inter} values employed were correct. The overall electrode mechanism was finally simulated by using the DigiSim software and the result compared to the experimental curves obtained in a wide scan rate range. Given the variety and quality of the complementary information in our hands, the k_{intra} values could be determined rather straightforwardly. The data are collected in Table 2.

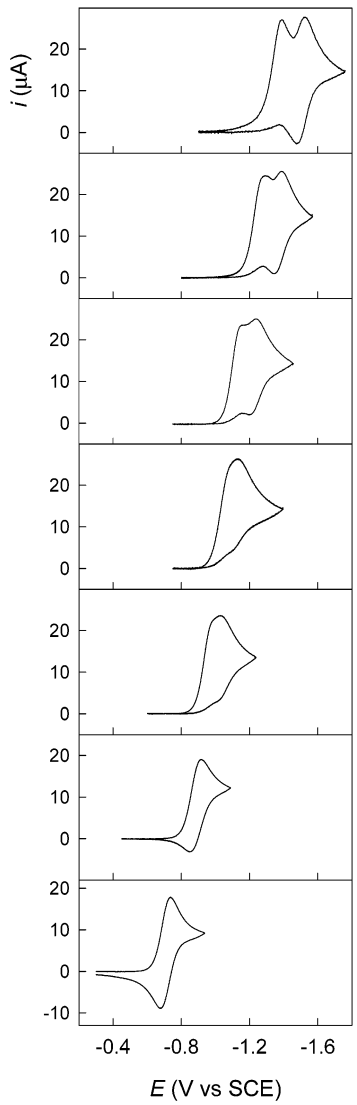

Figure 3. Comparison of the cyclic voltammograms of 1.0 mM **1a**−**g** (top to bottom) in DMF/0.1 M TBAP. Glassy carbon electrode, 0.2 V s^{-1}, and $T = 25$ °C.

In Figure 4, the intermolecular and intramolecular DET rate constants are compared as a function of the driving force. For the sake of comparison, the two sets of data were fit to a linear equation. There are two aspects of Figure 4 that are worth noting. First, the inter- and the intramolecular rate constant values display a slightly different dependence on the driving force, the slope of the log $k_{intra} - \Delta G°$ relationship being smaller than that of the log $k_{inter} - \Delta G°$ plot. It is noteworthy that this trend is completely different from and even slightly opposite to that previously reported for the intramolecular DET in the series of ring-substituted 4-benzoyloxy-1-methylcyclohexyl bromides (eq 4),[24] in which the intramolecular slope was significantly larger than that of the corresponding intermolecular

(35) Interestingly, when the same electrolysis was carried out in MeCN under otherwise identical conditions, 1 F mol^{-1} caused the disappearance of only 72% of the starting material. This is in agreement with the fact that MeCN is a poorer H-atom donor than DMF and thus with a nonnegligible contribution of the reduction of *t*BuO• to the overall electron consumption. This is consistent also with the detection of the oxidation peak of the conjugate base of acetanilide.

Table 2. Inter- and Intramolecular Rate Constant Values for Perester Reduction in DMF at 25°C.

1 or **3**	$\Delta G^{\circ a}$ (eV)	log k_{inter}[b,c] (M^{-1} s^{-1})	log k_{intra}[d] (s^{-1})
a	−1.207	5.23	3.80
b	−1.073	4.50	3.30
c	−0.935	3.85	2.70
d	−0.828	3.45	2.20
e	−0.739	2.90	1.85
f	−0.636	2.15	0.15
g	−0.469	1.38	−0.85

[a] E°(**2**) = −0.24 V. [b] Reaction of **3a**−**g** with **2**. [c] For comparison, we also measured the values for the reaction of **2** with the radical anions of methyl *p*-nitrobenzoate (E° = −0.875 V, log k_{hom} = 2.10) and *p*-cyanobenzaldehyde (E° = −1.323 V, log k_{hom} = 4.78). [d] Intramolecular dissociative ET in **1a**−**g**.

data. As mentioned in the Introduction, this result was attributed to the effect brought about by the electron-withdrawing properties of the substituent on the donor aryl ring. Therefore, on the basis of the present intramolecular data and above comparisons, it would appear that for **1a**−**e** the mild decrease of the intramolecular DET rate at low driving forces is caused by a progressive shortening of the effective D/A distance on going from **1a** to **1e**. The second aspect is the remarkably different behavior displayed by **1f** and **1g**. The k_{intra} values of **1f** and **1g** are 1.27 and 1.56 orders of magnitude smaller than those predicted by using the correlation of the sets of data of **1a**−**e**. Because of the well-known ability of nitro aromatics to act as ET acceptors, this trend can be easily attributed to a dramatic change of the LUMO of **1f** and **1g** with respect to **1a**−**e**. We will return to this point later.

Theoretical Calculations. Two types of ab initio MO calculations were carried out to gain more insight into the redox properties of our donor and acceptor systems and the problem of the effective distance suggested by the experimental kinetic analysis. First, we analyzed the donor SOMO to verify the effect of changing the substituents in the phenyl ring of the phthaloyl moiety. Calculations were carried out at MP2/6-311G*//HF/6-311G* and MP2/6-311+G*//HF/6-311G* levels. Since the focus was on the donor, we used the *N*-methylphthalimides **7a**−**d**

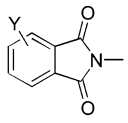

7

corresponding to our actual systems. The LUMO and the SOMO of **7a**−**d** and their radical anions have very similar features, as expected on the basis of the rigidity of the phthaloyl framework. The conversion of the neutral molecule into its radical anion is characterized by a reaction ΔG°, which is a function of the substituent. Although with different absolute values, the same dependence is calculated with and without inclusion of diffuse functions. Since the stability of the solvated radical anions increases with respect to the gas phase, the solvent has the effect of making the ΔG° values significantly more negative. Typically, while in the gas phase the ΔG° of **7a** at the MP2/6-311+G* level is −16.265 kcal mol^{-1}, the value obtained by simulating the presence of a medium having the dielectric constant of the solvent used for the electrochemical experiments (DMF, ϵ = 37) is −57.915 kcal mol^{-1}. With reference to the

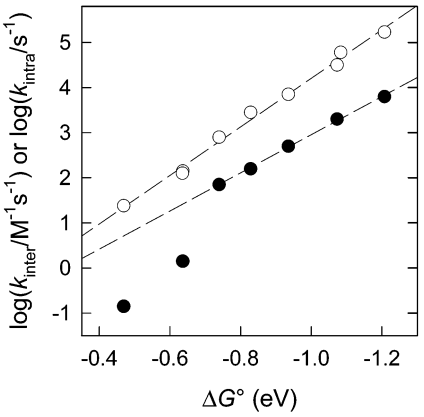

Figure 4. Logarithm of the first-order intramolecular (●) and the second-order intermolecular (○) ET rate constants for the reduction of the perester acceptor in **1a**−**g** or **2**, respectively, against the reaction free energy. The dashed lines are the linear fittings of the intramolecular (**1a**−**e**) or intermolecular data.

energy of **7a**, which is the least stabilized radical anion, the solvent-corrected ΔG° values of **7a**−**d** are $\Delta\Delta G^{\circ}$ = 0, −0.084, −0.325, and −0.356 eV, respectively. These values are linearly correlated to the electrochemical E°, the slope being 1.01 (r^2 = 0.935), which means that the correct structure of the radical anion was taken into account and that the difference between the solvation energy of the radical anion and that of the neutral molecule is kept constant along the series.[36] The behavior of the atomic charge distribution is particularly relevant in the frame of the present investigation. The charge densities of the entire pentatomic ring are as follows: **7a**, −0.943; **7b**, −0.983; **7c**, −1.010; **7d**, −1.037. In simple terms, these data would indicate that the SOMO moves a bit closer to the substituent at nitrogen when the E° of the donor becomes less negative. This finding is in agreement with the trend suggested by the ET data. A different picture, however, is associated with the nitro-substituted compound **7g**: Whereas the sum of the atomic charges on the pentaatomic ring is −0.532, that on the nitro group amounts to −0.969. Therefore, the SOMO of **7g** is very much localized onto the nitro substituent.

A second series of calculations was carried out to obtain more information about the ET properties of the acceptor. Here, we choose methylperacetate **8** as the model molecule. The energy

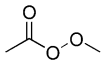

8

of a series of unoccupied orbitals was calculated at the HF/6-311G*//HF/6-311G* level as a function of the elongation of the O−O bond, all the other geometrical features being relaxed at each bond length value. Most of these orbitals do not change their energy appreciably, the most sensitive but still limited changes occurring for O−O bond length in the range 1.45−1.55 Å (Figure 5). However, for O−O distances larger than ∼1.55 Å, the LUMO1 starts decreasing its energy linearly and quite significantly (in the range 1.55−1.70 Å, the slope is −0.444 kcal $Å^{-1}$ and r^2 = 0.9999). Under these conditions, this orbital is clearly identified as the σ^* of the O−O bond, as

(36) (a) Kebarle, P.; Chowdhury, S. *Chem. Rev.* **1987**, *87*, 513. (b) Shalev, H.; Evans, D. H. *J. Am. Chem. Soc.* **1989**, *111*, 2667. (c) Ruoff, R. S.; Kadish, K. M.; Boulas, P.; Chen, E. C. M. *J. Phys. Chem.* **1995**, *99*, 8843.

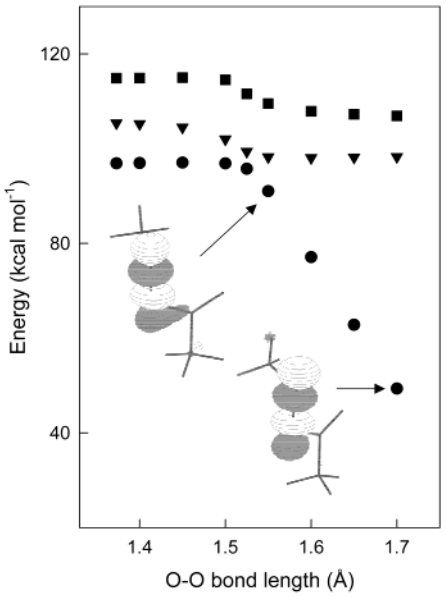

Figure 5. Energy of the first three unoccupied molecular orbitals (●, LUMO1; ▼, LUMO2; ■, LUMO3) of **8** as a function of the O−O bond length (HF/6-311G*//HF/6-311G* method). The σ^* character of the LUMO1, for distances in the range 1.55−1.70 Å, is also shown.

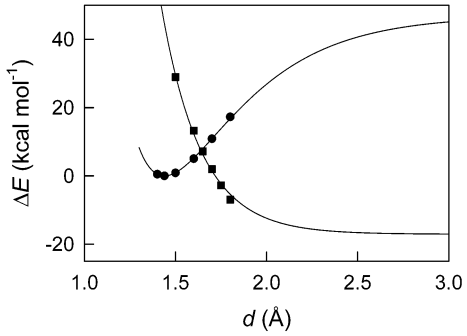

Figure 6. Energy profiles for the O−O bond cleavage of **8** and the fragments $MeCO_2^-$/MeO• as a function of the O−O distance. The calculations were carried out at the MP2/6-311G*//MP2/6-311G* level of theory. The data points (●, neutral molecule; ■, fragments) refer to the calculations at fixed O−O bond distances. The Morse curve was constructed by using the second derivative of the molecular energy with respect to the O−O bond distance. The exponential describing the reduction products is the best fit to the stationary-point data, including the energy of the fragments at infinite distance.

illustrated in Figure 5 for selected O−O bond distances. Therefore, once the thermal activation causes the O−O bond to elongate by ∼0.2 Å (at this level of theory, the calculated equilibrium O−O distance, d_0, is 1.373 Å), the molecule is set up for an efficient DET to take place.

We also calculated the Morse curve of **8** and the energy of the fragmentation products ($MeCO_2^-$ and MeO•) as a function of the O−O bond elongation (Figure 6). These calculations were carried out at the MP2/6-311G*//MP2/6-311G* level of theory, at which the O−O equilibrium distance is slightly longer than before ($d_0 = 1.439$ Å). The Morse curve of the neutral peroxide was constructed by using the second derivative of the molecular energy with respect to the O−O bond distance, according to a previously reported method.[37] We found the following values: BDE = 46.9 kcal mol^{-1}; $\beta = 2.52$ Å^{-1}. This BDE value is particularly large for a peroxide, although not too unexpectedly for this particular molecule.[38] On the other hand, the β value is in good agreement with that expected for alkyl peresters; in fact, an average $\beta = 2.8$ Å^{-1} can be calculated from the O−O stretching frequency (ν_0) of this class of compound, 854−858 cm^{-1},[7,39] using the relationship $\beta = \nu_0(2\pi^2\mu/\mathrm{BDE})^{1/2}$, where μ is the reduced mass.

A few calculations were carried out at different geometries along the nuclear coordinate for both the peroxide and the two fragments. The values of the neutral molecule were in excellent agreement with the corresponding values obtained from the Morse curve, as shown in Figure 6. Concerning the products, their energy is lower than that of the peroxide by 17.1 kcal mol^{-1}.[40] A decreasing exponential function such as $D\exp[-2\alpha(d - d_0)]$ could be used to fit the single-point results for O−O bond distances in the range 1.50−1.80 Å. This is qualitatively as expected on the basis of the Savéant's model of DET. On a quantitative ground, however, the fit did not match the exponential decay based on the repulsive part of the reactant Morse curve, i.e., BDE $\exp[-2\beta(d - d_0)]$. In fact, the best fitting parameters are $D = 61.7$ kcal mol^{-1} and $\alpha = 2.30$ Å^{-1}; if D is set equal to BDE as in the Savéant's model of DET, α becomes 1.67 Å^{-1} and thus even more different from the reactant's β, but the fit is poorer. In practice, the calculated data seem to overestimate the inner barrier relative to the simple DET model.

To summarize, our theoretical calculations support the concept that the aryl substituents affect the donor's SOMO and thus the charge distribution of the donor radical anion in the expected direction. Furthermore, the theoretical analysis points to a purely concerted DET to the perester O−O bond, leading directly to carboxylate and MeO• radical,[41] in qualitative agreement with the Savéant's model.

Intramolecular versus Intermolecular DET. According to the DET theory, the main ingredient contributing to the activation barrier is the energy associated with the stretching of the cleaving bond. Since according to the electrochemical results the simple DET model can be applied to the investigated systems, the $\Delta G_0^{\ddagger}$ can be calculated as $\Delta G_0^{\ddagger} = (\mathrm{BDE} + \lambda_S)/4$,[11a] in which λ_S is the solvent reorganization energy. The solvent reorganization energy of the intramolecular DET, which includes the distance effect caused by the spacer, was estimated to be 21.9 kcal mol^{-1}; the corresponding intermolecular DET

(37) Benassi, R.; Taddei, F. *J. Phys. Chem A* **1998**, *102*, 6173.

(38) The BDE of **8** was previously calculated to be in the range 37−47 kcal mol^{-1}, depending on the theory level and the introduction of spin annihilation and zero-point vibrational energy corrections: Benassi, R.; Taddei, F. *Tetrahedron* **1994**, *50*, 4795. These rather large values may be related to the difficulties of calculating the zero-point energy of σ alkoyl radicals at MP2 level of theory: Bach, R. D.; Ayala, P. Y.; Schlegel, H. B. *J. Am. Chem. Soc.* **1996**, *118*, 12758.

(39) (a) Vacque, V.; Sombret, B.; Huvenne, J. P.; Legrand, P.: Suc, S. *Spectrochim. Acta A* **1997**, *53*, 55. (b) Our own IR absorption measurements, carried out with **1a**−**e**, gave 856 cm^{-1}.

(40) The difference between the calculated energies of $MeCO_2$• and $MeCO_2^-$ (≡ BDE + 17.1 kcal mol^{-1}) provides a theoretical estimate of the gas-phase electron affinity of $MeCO_2$•. The result, 2.78 eV, is in fair agreement with available experimental data, which range from 3.07 to 3.40 eV: Bartmess, J. E. Negative Ion Energetics Data. In *NIST Chemistry WebBook*; Linstrom, P. J., Mallard, W. G., Eds.; NIST Standard Reference Database 69; National Institute of Standards and Technology, Gaithersburg MD, 20899, July 2001 (http://webbook.nist.gov).

(41) By extending the energy calculations to bond distances greater than 2.00 Å, the total molecular energy of the molecule reaches slightly lower values than the sum of the energies of the separate molecular fragments, which would point to the formation of a weak adduct anion−radical. At the level of theory employed, however, the characterization of this weak adduct as a stationary point failed owing to the large O−O bond distance considered and the swallow energy profile. In addition, the indication is that of a weak interaction, liable to vanish in solution.

value, calculated for contact D/A distance, is 15.9 kcal mol^{-1}.[42] Thus, the two $\Delta G_0^{\ddagger}$ values are 13.6 and 12.1 kcal mol^{-1}, respectively. Concerning the intermolecular reaction, the experimental k_{inter} data are in agreement with the theoretical prediction (eq 3), provided an average prefactor as small as 5×10^6 M^{-1} s^{-1} is used. The intramolecular process is also very slow, the average experimental prefactor being 1×10^6 s^{-1}. This outcome is in line with our recent findings concerning the nonadiabaticity of perester reduction.[6,7] The calculated prefactor is in agreement with the result of a temperature study that we carried out on the reaction between **2** and the radical anion of **3d**. In particular, the Arrhenius plot of the rate constant, obtained by using homogeneous redox catalysis at five temperatures in the range 240−317 K, led us to determine the remarkably low Arrhenius prefactor of 1×10^8 M^{-1} s^{-1}. Similar values were previously calculated for the homogeneous reduction of di-*tert*-butyl peroxide.[4c] The significance of the temperature coefficient of the DET to the perester acceptor will be discussed later.

From the slopes of the linear regression analyses of Figure 4, the symmetry factor α, which defines the sensitivity of the rate with respect to driving force variations and is given by $\alpha = -2.303RT\, \mathrm{d} \log k/\mathrm{d}\, \Delta G^{\circ}$, is calculated to be 0.286 and 0.250 for the inter- and the intramolecular rate constants, respectively. These α values pertain to the two corresponding series **2**/**3a**−**e** and **1a**−**e**. The intermolecular value, which is the average α value in the explored ΔG° range, is in agreement with the α values expected according to the DET quadratic activation/driving force relationship and thus to eq 12:

$$\alpha = \partial \Delta G^{\ddagger}/\partial \Delta G^{\circ} = 0.5 + \Delta G^{\circ}/8\Delta G_0^{\ddagger} \qquad (12)$$

The intermolecular α value corresponding to the midpoint of the ΔG° range, −0.973 eV, is 0.268. On the other hand, the prediction for the intramolecular value corresponding to the same ΔG° range is α = 0.294. It thus appears that the experimental intramolecular α value should have been observed only at smaller ΔG° values than those investigated; in particular, an α value of 0.250 would correspond (eq 12) to $\Delta G^{\circ} = -1.180$ eV. The difference, however, is pretty small. For comparison, the bromide systems (eq 3) gave a quite different result:[24] whereas the intermolecular data were in agreement with the theoretical expectation (midrange ΔG° value = −0.88 eV, α = 0.412), the α value of the intramolecular data was significantly larger, α = 0.510, which would have corresponded to $\Delta G^{\circ} = 0.08$ eV.

A comparison between the rate constant results obtained with **1a**−**g** and the **2**/**3a**−**g** systems is particularly useful to gain more insight into the intramolecular process. This is because of a series of useful facts and considerations: (i) the BDE and stretching frequency, and thus the Morse β, do not change with the remote phthaloyl group at the 4-position of the cyclohexane perester molecule; (ii) the reaction free energy of the intramolecular and corresponding intermolecular systems is the same; (iii) in **1a**−**g**, the D/A orientation is the same, also because the conformational mobility of these molecules is expected to be independent of the aryl substituent; (iv) there are no reasons to believe that the average distance and orientation in the reactions of **2** with **3a**−**g** should depend on the phthaloyl substituents; (v) given the similarity of the reacting molecules, the equilibrium constant of the diffusion-controlled formation of the caged D/A reacting system, K_d,[43] may be taken as constant within the series. Therefore, once diffusion is taken into account, the difference between the corresponding k_{intra} and k_{inter} ($k_{inter} = K_d k^{\ddagger}_{inter}$, in which $k^{\ddagger}_{inter}$ is the actual first-order rate constant for the reaction of **2** with **3a**−**g** in the solvent cage) is attributable only to the solvent reorganization energy and the D/A electronic coupling integral H_{DA}.

The first-order DET rate constant (either k_{intra} or $k^{\ddagger}_{inter}$) is conveniently expressed in terms of the nonadiabatic DET theory of German and Kuznetsov.[44] By applying this theory, a deeper understanding of the parameters affecting the magnitude of the prefactor of the rate constant expression can be obtained. Because of its relative simplicity, it is particularly useful to employ the semiclassic limit of the theory. In this limit, whereas the harmonic approximation is used for the intramolecular vibrations and the solvent polarization, the breaking bond is viewed as ruled by a Morse potential. The prefactor of the rate constant expression results to be proportional to H_{DA}^2 and to be a function of both $\Delta G_0^{\ddagger}$ and the bond elongation at the transition state, $d^{\ddagger} - d_0$. According to our present and previous[5−7] experimental results, the Savéant's model,[11b] in which the potential energy describing the products is simply taken as the repulsive part of the Morse curve of the reagents, provides a simple and efficient way to describe the nuclear factor of the DET to peroxides. By this approach, the nonadiabatic rate constant expression (k is either k_{intra} or $k^{\ddagger}_{inter}$) is as shown in eq 13 in which the bond elongation is a function of both

$$k = (2\pi/\hbar)(H_{DA})^2\{16\pi RT\, \Delta G_0^{\ddagger} \exp[-2\beta(d^{\ddagger} - d_0)]\}^{-1/2} \exp(-\Delta G^{\ddagger}/RT) \qquad (13)$$

$\Delta G_0^{\ddagger}$ and ΔG°, being $\beta(d^{\ddagger} - d_0) = \ln 2 - \ln(1 - \Delta G^{\circ}/4\Delta G_0^{\ddagger})$.[45] We used this method to estimate the electronic coupling term H_{DA} for both the inter- and intramolecular rate constants, leading to average H_{DA} values of 0.45 (systems **2**/**3a**−**g**) and 0.095 cm^{-1} (systems **1a**−**e**), respectively. In both series, corresponding to a driving force variation of 0.74 and 0.47 eV, respectively, the values are equal to within 20%.

The temperature study carried out with the system **2**/**3d** provides further support to this outcome. According to eq 13, the function $\ln(kT^{1/2})$ should be linear with respect to $1/T$, provided $\Delta G_0^{\ddagger}$ and ΔG° are constant in the explored T range. The plot was indeed sufficiently linear ($r^2 = 0.995$) to allow us to extract meaningful parameters from the slope and the intercept. From the slope, using the appropriate ΔG°, we could calculate $\Delta G_0^{\ddagger} = 14.4$ kcal mol^{-1}. This value is in reasonable

(42) The λ_S value was estimated by using the empirical equation $\lambda_S = 95[(2r_D)^{-1} + (2r_A)^{-1} - (R_{DA})^{-1}]$,[4c] where r_D and r_A are the donor and acceptor radii, 3.4 and 2.72 Å, respectively, and R_{DA} is the D/A distance. The latter term is taken as either equal to $r_D + r_A$ or to $r_D + r_A + r_{Sp}$, where r_{Sp} is the edge-to-edge distance of the *cis*-1,4-cyclohexanedyil, 3.9 Å.

(43) K_d can be calculated by using the equation $K_d = [(4\pi N r^2 \delta r)/1000]$ (Sutin, N. *Prog. Inorg. Chem.* **1983**, *30*, 441), taking advantage of the fact that **2** is uncharged. The DET is viewed as occurring significantly only between the contact distance r (taken as the van der Waals distance $r_D + r_A$) and $r + \delta r$, in which δr ranges from ∼2 to ∼0.3 Å for adiabatic and nonadiabatic reactions, leading to $K_d = 5.7 \times 10^{-1}$ and 8.5×10^{-2} M^{-1}, respectively. Since the reduction of alkyl peresters is strongly nonadiabatic,[7] we employed the latter value.

(44) (a) German, E. D.; Kuznetsov, A. M. *J. Phys. Chem.* **1994**, *98*, 6120. (b) German, E. D.; Kuznetsov, A. M.; Tikhomirov, V. A. *J. Phys. Chem.* **1995**, *99*, 9095.

(45) In refs 4c and 7, the exponential term of the prefactor (eq 13) was erroneously typed as $\exp[-\beta(d^{\ddagger} - d_0)]$.

agreement with our estimate of 12.1 kcal mol^{-1}; interestingly, if the solvent reorganization energy is calculated by using the Marcus approach,[1a] $\Delta G_0^{\ddagger}$ is estimated to be 14.5 kcal mol^{-1}, which is an even closer value to the temperature study result. From the intercept, using the experimental $\Delta G_0^{\ddagger}$, H_{DA} is calculated to be 0.80 cm^{-1}, in satisfactory agreement with the above-mentioned average value of 0.45 cm^{-1}.

The intramolecular H_{DA} values of **1a**−**e** tend to increase steadily when the driving force decreases: 0.081 (**1a**), 0.088 (**1b**), 0.093 (**1c**), 0.099 (**1d**), and 0.115 cm^{-1}(**1e**). Therefore, since k_{intra} is proportional to $(H_{DA})^2_{intra}$, it follows that according to this effect the prefactor increases by a factor 2 on going from **1a** to **1e**. The rate-enhancing effect caused by the increase of the O−O bond distance at lower driving force, which affects k through the term $\exp[-2\beta(d^{\ddagger} - d_0)]$, is less significant, corresponding to a factor 1.15 (**1a** → **1e**). Although this trend of k_{intra} would be consistent with the theoretical results on the donor SOMOs, the variation is indeed small and thus we can conclude that the nonadiabatic intramolecular DET in compounds **1a**−**e** is in agreement, within error, with the DET model. The less steep slope of the intramolecular data relative to the intermolecular counterpart (cf. Figure 4) is thus caused, to a large extent, by the distance effect on the solvent reorganization energy. For our systems, λ_S increases typically by ∼40% on going from the intermolecular to the intramolecular value. This variation affects the curvature of the quadratic activation/driving force relationship accordingly.

Quantitative prediction of the intramolecular rate, however, is possible only if the donor and acceptor orbitals are kept essentially unaffected by driving force variations; in fact, although approximately verified for **1a**−**e**, which were purposely devised to fulfill the latter requirement, a reliable prediction was not possible with the already mentioned bromide systems.[24] The results obtained with the two nitro-substituted compounds provide the final proof. We have seen both experimentally (**1f** and **1g**) and theoretically (**7g**) that the nitrophthaloyl derivatives behave differently from the other systems investigated. Since for **1f** and **1g** the effective distance between the donor and acceptor orbitals is larger than for **1a**−**e**, H_{DA} decreases and the solvent reorganization increases. Both factors contribute to the significant decrease of the k_{intra} of **1f** and **1g** (1.27 and 1.56 orders of magnitude) from the values expected in comparison with the data of **1a**−**e**. On the other hand, the intermolecular rates are perfectly in line with the results obtained with the other donors, meaning that k_{inter} is determined only by the $E°$ of the nitro derivative. This is because the intermolecular rate is a consequence of random distance and orientation distributions in the encounter complex.

In conclusion, the outcome of the present investigation fully confirms the hypothesis made on the occasion of our first study on intramolecular DETs.[24] In particular, our results show that the DET rate constants of intramolecular processes, within the limits of the theory and by taking into account distance and λ_S differences, are at least as predictable as the corresponding k_{inter} values. We expect to be now in a position of understanding and even predicting the values of the rate constants of intramolecular dissociative-type processes, particularly in view of possible applications concerning biologically relevant molecular systems bearing the O−O and S−S bonds.

Experimental Section

Chemicals. Compounds **1a**, **2**, **3a**, and **4a** were available from a previous study.[7] The mediators other than **3a**−**g** were commercially available and used as received. *cis*-4-Aminocyclohexanecarboxylic acid was purchased from Fluka. The phthalic anhydrides were purchased from Aldrich. The syntheses of **1b**−**g**, **3b**−**g**, and **4b**−**g** were carried out along the general lines described below. Full synthetic details and description of the methods are provided in the Supporting Information.

The *N*-phthaloylated cyclohexanecarboxylic acids **4** were prepared in good yields (∼80%) according to the procedure described by Gabriel,[46] i.e., by melting the corresponding phthalic anhydride in the presence of *cis*-4-aminocyclohexanecarboxylic acid. Except for **4e**, for which the reaction was carried out in acetic acid,[47] the synthesis of the other acids was carried out in the absence of solvent. After workup, the N-phthaloylated acids were obtained in a chromatographically homogeneous state by recrystallization. These derivatives were dissolved in CH_2Cl_2 and the corresponding peresters **1b**−**g** prepared in 40−75% yield by activating the carboxylic function with *N*-ethyl-*N*′-dimethylaminopropyl carbodiimide in the presence of equimolar amounts of *tert*-butyl hydroperoxide and 4-(dimethylamino)pyridine (catalyst). The progressive conversion to the perester was conveniently monitored by selective visualization of the O−O bond, achieved by developing the TLC plates with a solution of NH_4SCN and $FeSO_4 \cdot (NH_4)_2SO_4 \cdot 6H_2O$ (Mohr's salt) in 1% H_2SO_4. By replacing *tert*-butyl hydroperoxide with methanol, the same activation procedure was used to prepare the N-phthaloylated methyl esters **3b**−**g** in good yields (∼80%).

Electrochemical Apparatus and Procedures. *N*,*N*-Dimethylformamide (Acros Organics, 99%) was treated for some days with anhydrous Na_2CO_3, under stirring, and then distilled at reduced pressure (17 mmHg) under a nitrogen atmosphere. Acetonitrile (BDH) was distilled over CaH_2 and stored under an argon atmosphere. The supporting electrolyte was tetrabutylammonium perchlorate (99%, Fluka) that was recrystallized from a 2:1 ethanol/water solution and dried at 60 °C under vacuum. Electrochemical measurements were conducted in an all-glass cell, thermostated at 25 °C. An EG&G-PARC 173/179 potentiostat-digital coulometer, an EG&G-PARC 175 universal programmer, a Nicolet 3091 12-bit resolution digital oscilloscope, and an Amel 863 X/Y pen recorder were used. The feedback correction was applied to minimize the ohmic drop between the working and the reference electrodes. Experiments were carried out inside a double-wall copper Faraday cage.

For cyclic voltammetry measurements, glassy carbon was the working electrode. The electrode was prepared and activated before each measurement as previously described.[4b] The electrode area was determined through the limiting convolution current of ferrocene, the diffusion coefficient of ferrocene being 1.13×10^{-5} cm^2 s^{-1} in DMF. The reference electrode was Ag/AgCl, calibrated after each experiment against the ferrocene/ferricenium couple. All potentials were converted to the KCl saturated calomel electrode (SCE) by using $E°_{Fc/Fc^+} = 0.464$ V versus SCE. The counter electrode was a 1-cm^2 Pt plate. The reference electrode and the counter electrode were separated from the catholyte by glass frits and Tylose-TBAP-saturated bridges. Controlled-potential electrolyses were carried out in a divided cell by using a large surface area Pt grid.

Voltammetric analyses were carried out on low-noise voltammetric curves, recorded according to a procedure previously described.[4b] In the experiments involving the reduction of the perester function, a small amount of acetanilide was added to the solution to hamper the father-son reaction between **1** and *t*BuO$^-$.[6] The digitalized, background-subtracted curves were analyzed by using our homemade voltammetry−convolution software and compared with the corresponding digital

(46) Gabriel, S. *Ber. Dtsch. Chem. Ges.* **1911**, *44*, 57.
(47) El-Naggar, A. M.; Zaher, M. R.; Salem, A. A. *Int. J. Pept. Protein Res.* **1982**, *20*, 1.

simulations. The DigiSim 3.03 package was used for the simulations, using a stepsize of 1 mV and an exponential expansion factor of 0.5.

Controlled-potential electrolysis was carried out under vigorous magnetic stirring in a solution (DMF or MeCN, 20 mL, containing 0.1 M TBAP) containing the starting molecule, **1a**, at 9 mM concentration. One equivalent of acetanilide was also present in the solution. After selected amounts of electricity were allowed to flow in solution (0.25, 0.50, and 0.75 F mol^{-1}), the extent of electrolysis was checked by cyclic voltammetry and GC/mass spectrometry analysis of solution samples. After 1 F mol^{-1}, methyl iodide (2 equiv) was added to the solution to trap the carboxylate anion. The alkylation is quantitative, as verified in separate experiments with authentic solutions of deprotonated **4a**. The electrolyzed solution was analyzed by GC/mass spectrometry, using a Hewlett-Packard 6890 gas chromatograph equipped with a 5973 mass-selective detector. An HP-5MS 30-m, 0.25-mm-i.d. GC column was used. The injection temperature was 200 °C and the helium flow 0.8 mL min^{-1}. The temperature was initially at 50 °C for 3 min and then increased to 280 °C at 10 °C min^{-1}. Quantitative information was obtained in comparison with calibration curves constructed with authentic samples of **1a** and **3a**. In DMF, **3a** was the only detectable product; its fragmentation pattern is as follows: MS (EI) *m*/*z* (%) 287 (M^+, 13), 256 (13), 228 (9), 227 (8), 212 (7), 186 (38), 173 (26), 160 (13), 149 (13), 148 (82), 142 (20), 140 (100), 130 (43), 108 (42), 104 (18), 81 (20), 80 (41), 76 (14). Concerning the electrolysis in MeCN, carried out and analyzed as for the DMF solution, 28% of **1a** was still detectable after passage of 1 F mol^{-1}.

X-ray Diffraction. Colorless single crystals of **1a**, **1b**, and **1c** were grown from chloroform/light petroleum by vapor diffusion, acetone/water by slow evaporation, and acetonitrile by slow evaporation, respectively. Cell parameters were obtained by least-squares refinement of the angular setting of 25 carefully centered reflections in the 12−20° θ range. Data collections were performed with a Philips PW1100 four-circle diffractometer, using graphite-monochromated Cu Kα radiation, in the θ-2θ scan mode up to $\theta = 60°$. The three structures were solved by direct methods of the SHELXS 97 program.[48a] Refinement was carried out on F^2, using the full data set and the SHELXL 97 program[48b] with all non-H atoms anisotropic. In the asymmetric unit of **1b**, two independent molecules (**A** and **B**) are present. The *t*Bu group of molecule **B** is disordered. It was refined on two sets of positions, each with a population parameter of 0.5. Restraints were applied to the bond distances and bond angles involving the disordered atoms. Some rotational disorder is also likely at the level of the *t*Bu group in **1c**, as indicated by the large anisotropy of its methyl carbon atoms. However, in this case, the data did not support a viable model to unravel such disorder satisfactorily. Restraints were applied to the bond distances as well to the anisotropic displacement parameters of the atoms belonging to the *t*Bu group. H-Atoms were calculated at idealized positions and refined as riding, with U_{iso} set equal to 1.2 (or 1.5 for the CH_3 groups) times the U_{eq} of the parent atom. Other relevant crystallographic data and structure refinement parameters are listed in the Supporting Information.

(48) (a) Sheldrick, G. M. *SHELXS 97. Program for the Solution of Crystal Structures*; University of Göttingen: Göttingen, Germany, 1997. (b) Sheldrick, G. M. *SHELXL 97. Program for Crystal Structure Refinement*; University of Göttingen: Göttingen, Germany, 1997.

Computational Details. All the calculations were performed with the Gaussian-98 series of programs,[49] run on a Silicon Graphics 4CPU MIPS R10000. Different levels of theory were adopted, depending on the complexity of the molecules examined. Conformational analysis for **5** and **6** was carried out at the HF/6-31G*//HF/6-31G* level, and beside the conformation of absolute minimum the energy of two conformations with frozen torsional angle referred to the exocyclic C−C bond to the peroxy ester were also calculated. For the series of substituted *N*-methylphthalimides **7a**−**c**, correlation effects were calculated with the frozen core (fc) second-order Møller−Plesset perturbative treatment.[50] For **8**, its radical anion, acetyl radical and acetyl anion, and methoxy radical, total molecular energy was calculated at the MP2/6-311G*//MP2/6-311G* level. The total molecular energy of **8** and of its radical anion as a function of O−O bond elongation refers to the same level of theory: for a number of frozen distances, the total molecular energy was calculated by relaxing all the other geometrical parameters. UHF wave functions were employed for the open-shell systems, and the spin-projection operator[51] was applied in order to remove contamination for higher spin states (results are reported as PMP2 values). The values of $<s^2>$ from the different approaches reduced to values close to 0.75 after spin projection. Harmonic frequency calculations were also carried out in the stationary points. Solvent effects were estimated through the Self-Consistent Reaction Field (SCFR) facility employing the polarized continuum model (PCM) performed with the Onsager reaction field model, implemented on the Gaussian 98 package. Thermodynamic data refer to 298.15 K.

Acknowledgment. This work was financially supported by the University of Padova (research project A.0EE00.97) and the Ministero dell'Istruzione, dell'Università e della Ricerca (MIUR).

Supporting Information Available: Optimized geometries and energies for all the stationary points discussed in the text, crystallographic data of **1a**−**c**, and synthesis and characterization of compounds **1b**−**g**, **3b**−**g**, and **4b**−**g**. This material is available free of charge via the Internet at http://pubs.acs.org.

JA0263644

(49) Gaussian 98, Revision A.7. Frisch, M. J.; Trucks, G. W.; Schlegel, H. B.; Scuseria, G. E.; Robb, M. A.; Cheeseman, J. R.; Zakrzewski, V. G.; Montgomery, Jr., J. A.; Stratmann, R. E.; Burant, J. C.; Dapprich, S.; Millam, J. M.; Daniels, A. D.; Kudin, K. N.; Strain, M.; Farkas, C. O.; Tomasi, J.; Barone, V.; Cossi, M.; Cammi, R.; Mennucci, B.; Pomelli, C.; Adamo, C.; Clifford, S.; Ochterski, J.; Petersson, G. A.; Ayala, P.; Cui, Y. Q.; Morokuma, K. D.; Malick, K.; Rabuck, A. D.; Raghavachari, K.; Foresman, J. B.; Cioslowski, J.; Ortiz, J. V.; Baboul, A. G.; Stefanov, B. B.; Liu, G.; Liashenko, A.; Piskorz, P.; Komaromi, I.; Gomperts, R.; Martin, L. R.; Fox, D. J.; Keith, T.; Al-Laham, M. A.; Peng, C. Y.; Nanayakkara, A.; Gonzalez, C.; Challacombe, M.; Gill, P. M. W.; Johnson, B.; Chen, W.; Wong, M. W.; Andres, J. L.; Gonzalez, C.; Head-Gordon, M.; Replogle, E. S.; Pople, J. A.. Gaussian, Inc., Pittsburgh, PA, 1998.

(50) (a) Møller C.; Plesset, M. S. *Phys. Rev.* **1934**, *46*, 618. (b) Here, W. J.; Radom, L.; Schleyer, P. V.; Pople, J. A. *Ab-initio Molecular Orbital Theory*; Wiley: New York, 1986.

(51) (a) Schlegel, H. B. *J. Chem. Phys.* **1986**, *84*, 4530. (b) Schlegel, H. B. *J. Phys. Chem.* **1988**, *92*, 3075. (c) Sosa, C.; Schlegel, H. B. *Int. J. Quantum Chem.* **1986**, *30*, 55.